Nanofluid sprays for cooling applications

M. Malý[1], A.S. Moita*[2], J. Jedelsky[2], A.P.C. Ribeiro[3], A.L.N. Moreira[2]
[1] Faculty of Mechanical Engineering, Brno University of Technology, Brno, Czech Republic.
[2] IN+ - Center for Innovation, Technology and Policy Research, Instituto Superior Técnico, Universidade de Lisboa, Lisboa, Portugal.
[3] Centro de Química Estrutural, Instituto Superior Técnico, Universidade de Lisboa, Lisboa, Portugal.
*Corresponding author: anamoita@tecnico.ulisboa.pt

Introduction

Spray cooling is among the most popular liquid cooling strategies, given the high heat transfer coefficients that can be delivered [1]. However, increasingly demanding heat loads in applications such as electronics cooling have pushed researchers to further enhance the heat transfer processes, by altering the surfaces and/or the fluids e.g. [2-4]. Fluids with nanoparticles are pointed to have great potential to improve heat transfer processes, given their potentially higher thermal properties. However, increasing the concentration of the nanoparticles may alter significantly other physical properties such as the viscosity, which affect the fluid flow and may eventually reverse any advantage of adding the nanoparticles. Furthermore, while most authors have focused simply on the effect of the nanoparticles on the bulk properties of the fluid, studies on the wettability and on the interaction effects of the particles on the surfaces and on droplet-droplet interactions is scarcely reported. The actual effects of adding nanoparticles in the fluid flow characteristics and, particularly in the mechanisms of atomization, have also been drawn to a secondary plane.

In this context, the present work focuses on the effect of nanofluid preparation, particularly on the effect of the nanoparticles concentration, on the local physical properties of the resulting fluid and their consequent effect on the atomization characteristics (droplet size, velocity distribution, spray angle, etc) using nanofluids. The results are discussed focusing on how the spray characteristics affect the use of the resulting spray for cooling purposes. Nanoparticles of alumina (Al_2O_3) and Zinc Oxide (ZnO) are mixed in water-based solutions, for concentrations varying between 0.5% and 2% wt for alumina and between 0.01% and 0.1% wt for the zinc oxide particles. CuO (0.1% wt) and $FeCl_2.4H_2O$ (0.1% wt) were also used to infer on the effect of the nature (material) of the particles in the physico-chemical properties of the resulting solutions. High-speed imaging is combined with Phase Doppler Anemometry and Laser Scanning Confocal Microscopy to fully characterize the nanofluids properties and the spray characteristics.

The results show that liquid viscosity is an important parameter in predetermining the spray characteristics of the nanofluids, as it affects the primary breakup. However, only a minor increase is observed in the nanofluids viscosity, mainly for higher concentrations of alumina. This variation in the viscosity was observed to slightly affect droplet size distribution and to cause a small decrease in the cone angle of the spray. Hence, for the range of nanoparticles nature and concentration covered here, there is a positive balance in the use of the nanoparticles, increasing the thermal properties without a significant deterioration of other fluid properties such as viscosity, or spray dynamics.

Material and methods

The sprays are generated in a small pressure-swirl type atomizer, with a square cross-section 0.6 x 0.6 mm, which produces a wide cone spray. The discharge orifice is 0.42 mm.

The liquid is supplied from a small (3 l) pressure vessel, pressurized by air at 87 PSI. At this pressure (approx. 5 bar overpressure), the mass flow rate through the atomizer is approx. 7 kgh^{-1}.

The nanofluids are prepared following a two-step process. The particles are mixed with DI water, in concentrations ranging between 0.01 and 2% weight percentages and placed in an ultrasonic bath for 1 h. The specific nanofluid concentrations used in the present work are identified in Table 1. Citric acid was added as a surfactant, to maintain the particles dispersed and the nanofluids stable during the experiments. The nanoparticles are mainly composed by metals and oxide metals to enhance the thermal properties of the resulting nanofluids, for cooling applications.

The wettability of the nanofluids on the contact surfaces was quantified by equilibrium contact angles, using an optical tensiometer (THETA from Attension). Uncertainty of the contact angle measurements was at most of the order of ±5º.

The measurements were performed following the sessile droplet method, as detailed, for instance in [5]. In addition, a Laser Scanning Confocal Microscope (Leica SP8) was used to perform Laser Scanning Confocal Fluorescence

Microscopy – LSCFM - and 3D reconstruction, to visualize the micro-layer in the very vicinity of the triple contact line and characterize wettability within improved spatial resolution, as in [6].
As for the properties of the nanofluids, density was evaluated from the solutions concentration, by mass conservation principles and was very close to that of the water (DI) for all the samples tested (ρ = 998kgm^{-3}). The viscosity was measured with an ATS RheoSystems (a division of CANNON® Instruments, Co) under controlled temperature conditions, with an accuracy of ±5%. Finally, the surface tension was measured under controlled temperature conditions (20 ± 2ºC) with an optical tensiometer THETA (Attention), using the pendant drop method. The value taken for the surface tension of each solution was averaged from 15 measurements, with a maximum standard deviation of the mean of 0.04 mNm^{-1}.

Table 1. Composition and main physico-chemical properties of the nanofluids used in the present study.

Sample number	Weight percentage (wt %)					Size of the particles [nm]	μ_l gm^{-1}s^{-1}	σ_{lv} mNm^{-1}
	Surfactant		Oxide		Deionized water			
1	Oleic acid	0.15	---		99.85 (pure)		1.02	74.2
2	Citric acid	0.15	Al_2O_3	2	97.85 (pure)	80	1.12	72.8
3	Citric acid	0.15	Al_2O_3	0.5	99.35 (pure)	80	1.05	73.4
4	Citric acid	0.15	ZnO	0.5	99.35 (pure)	80	1.02	74.3
5	Citric acid	0.15	ZnO	0.01	99.84 (pure)	80	1.28	73.0
6	Citric acid	0.15	CuO	0.1	99.75 (pure)	50	1.05	72.0
7	Citric acid	0.15	$FeCl_2$. $4H_2O$	0.1	99.75 (pure)	≥ 100	1.04	71.6

The spray was characterized combining high-speed imaging with phase Doppler anemometry measurements.
A Phantom v4.2 high-speed camera was used to obtain spray images, which were afterwards post-processed to analyse qualitatively the morphology of the sprays and to evaluate several additional parameters such as the spray cone angle. Images were taken at 15kHz, with a resolution of 192x192px^2.
Phase Doppler measurements were performed with a two-component system from Dantec, to describe size and velocity distributions in the resulting nanofluid sprays.
A measurement grid was used which considers a radial system, as defined in Figure 1, where r = 0mm corresponds to the center of the spray cone and z=0mm is at the exit of the spray nozzle. Measurements were performed for -20mm < r < 20mm, -20mm < y < 20mm and z = 10mm and Z = 20mm, in 2mm steps for each direction.
Detailed description of the experimental arrangement and of the measurement procedures is provided in [3].

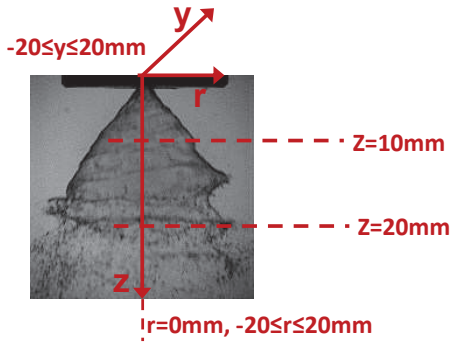

Figure 1. System of coordinates used in the measurements with the phase Doppler instrument.

Results and Discussion
Table 1 does not evidence significant differences between the surface tension values measured for the different nanofluid solutions. The viscosity, on the other hand, is observed to increase mildly, even for the low nanoparticle

concentrations used here. It is worth mentioning that the properties of the solutions were measured before and after atomization, to check on the stability of the solutions and on the possible effect of particles trapping in the atomizer in the liquid feeding system, which could alter the real concentration of the solutions and, consequently their physico-chemical properties. Any significant changes were observed in the measurements performed before and after the atomization. This slight increase in the bulk viscosity of the nanofluids was therefore further investigated to infer how it could be affecting the spray atomization processes. In line with this, the morphology of the various nanofluid sprays was observed from high-speed imaging. Image analysis and post-processing reveals no significant different between the morphology of the various nanofluid sprays. Also, the liquid sheet breakup length, evaluated based on these images was observed to occur at about 5–7 mm below the exit orifice, independently from the nanofluid used. Based on these observations, a more careful analysis was performed at two main axial distances from the nozzle, namely at z=10mm and z=20mm. While at the distance closer to the exit orifice the measurements are performed just after the primary breakup, which is definitly more affected by the liquid viscosity, the measurements performed at z=20mm may be less affected by viscosity, being therefore expected to be dominated by surface tension effects. Such relative dominance of viscous vs surface tension effects can be discussed, observing the spray cone angle and the integral Sauter mean diameter ID_{32}, as defined by [7], as a function of the dynamic viscosity, which in turn increases with the concentration of the nanoparticles, as obseved in Table 1.

Hence, the spray cone angle measurements performed at z=10mm, as depicted in Figure 2a show a small decline with increasing viscosity, evidencing a dominant effect of the viscous forces. This maybe so, since larger viscosity tends to promote dissipation inside the swirl chamber of the atomizer, thus lowering the flow velocities and consequently, decreasing the spray cone angle. However, as the measurements are performed farther away from the primary breakup region, the viscosity effect becomes negligleable, thus suggesting the dominance of the surface tension, which is hardly affected by the presence of the nanoparticles (Figure 2b).

These trends are supported by measurements of ID_{32}, also represented as a function of the nanofluids viscosity. Again, the effect of increasing the viscosity of the nanofluids, caused by the addition of the nanoparticles leads to a mild increase in the ID_{32} (Figure 3a) at the primary break-up region (z =1 0mm), which is hardly noticed at z = 20mm (Figure 3b).

The ratio between the liquid phase Weber and Reynolds numbers at z = 20mm, roughly varies between 0.35 and 0.5, depending on the nanofluid used, thus reinforcing the trend that the increasing concentration of the nanofluids strongly affects the region of the primary break-up, which is governed by the increased viscous forces, but has only a minor effect as the spray becomes fully developed.

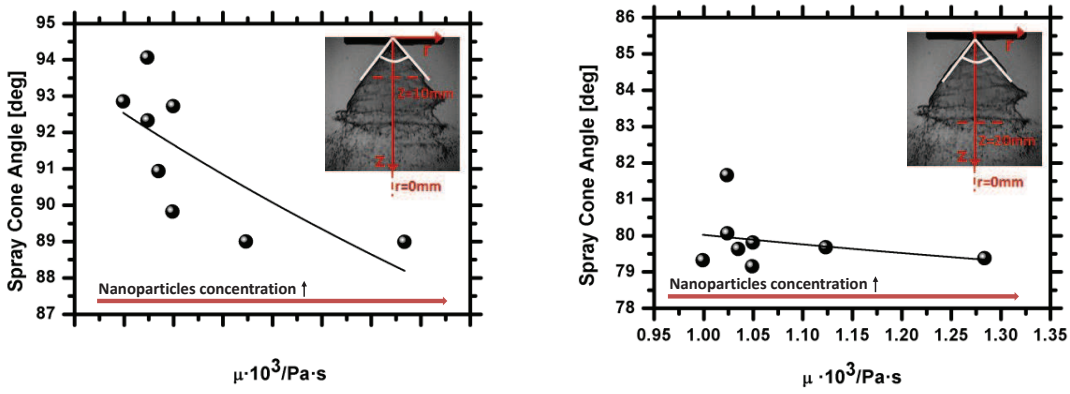

a) b)

Figure 2. Effect of the nanoparticles concentration (represented in the nanofluids viscosity) on the spray cone angle at a) z = 10 mm. b) *z* = 20 mm.

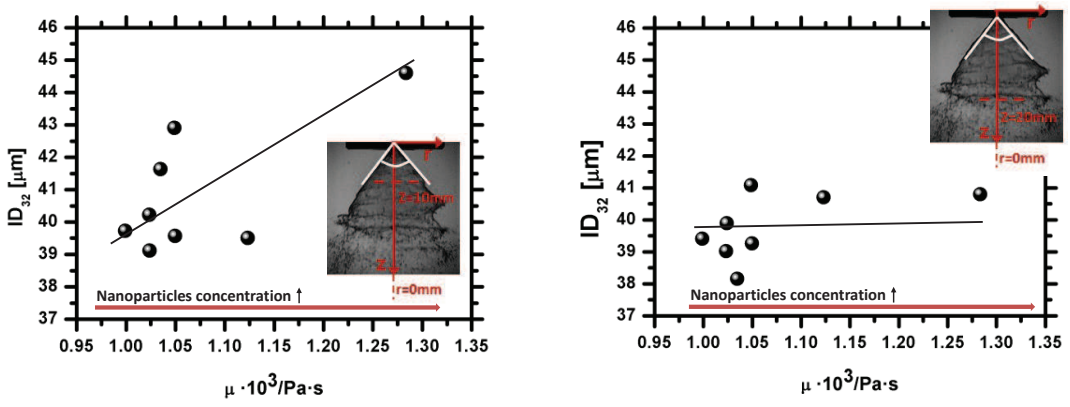

Figure 3 Effect of the nanoparticles concentration (represented in the nanofluids viscosity) on the characteristic size of the spray droplets. PDA measurements performed at a) z = 10 mm. b) z = 20 mm.

Conclusions

This work addresses the effect of nanoparticles concentration on the atomization processes of the resulting nanofluid sprays, to be used in the context of cooling applications.

Additional investigation is now required to widen the range of nanoparticles concentration and to study the spray dynamics and the heat transfer processes at imingement. However, these results are rather encouraging to use these nanoparticles for spray coooling applications, as they are able to enhance the thermal properties of the nanofluids without significantly compromising the spray characteristics, as the atomization processes in the fully developed region of the spray are mostly dominated by surface tension forces, which are hardly affected by the concentration of the nanoparticles.

Acknowledgements

This work has been partially supported by project No. 18-15839S funded by the Czech Science Foundation.

The authors are also grateful to Fundação para a Ciência e Tecnologia (FCT) for partially financing the research under the framework of the project RECI/EMS-SIS/0147/2012 and for supporting M. Maly with a research fellowship, during his stage at IN+. A. S. Moita acknowledges FCT for financing her contract and exploratory research project through the recruitment programme FCT Investigator (IF 00810-2015).

References

[1] Moreira, A.L.N., Moita, A.S., Panão, M.R., Prog. Energy Combustion Sci. 36:554-580 (2010).

[2] Kim, J., Int. J. Heat Fluid Flow 28(4):753-767.

[3] Maly, M., Moita, A.S., Jedelsky, J., Ribeiro, A.P.CP., Moreira, A.L.N., J. Thermal Analysis Calorimetry, In press (published online 12 June 2018).

[4] Duursma, G., Sefiane, K., Kennedy, A., Heat Transf. Eng. 30(13):1108-1120.

[5] Pererira, P., Moita, A.S., Monteiro, G., Prazeres, D.M.F., J. Bionic Eng. 11(3):436-259 (2014).

[6] Vieira, D., Moita, A.S., Moreira, A.L.N., 18th International Symposium on Applications of Laser and Imaging Techniques to Fluid Mechanics. Lisbon, Portugal, 04-07 July, 2016.

[7] Jedelsky, J. Jicha, M., App. Energy 132:485-495 (2014).